What is Solvatochromism?

Alberto Marini, Aurora Muñoz-Losa, Alessandro Biancardi, and Benedetta Mennucci*

Dipartimento di Chimica e Chimica Industriale, Università di Pisa, Via Risorgimento 35, 56126 Pisa, Italy

Received: October 11, 2010; Revised Manuscript Received: November 16, 2010

Solvatochromism is commonly used in many fields of chemical and biological research to study bulk and local polarity in macrosystems (membranes, etc.), or even the conformation and binding of proteins. Despite its wide use, solvatochromism still remains a largely unknown phenomenon due to the extremely complex coupling of many different interactions and dynamical processes which characterize it. In this study we analyze the influence of different solvents on the photophysical properties of selected charge-transfer probes (4-AP, PRODAN, and FR0). The purpose is to achieve a microscopic understanding of the intermolecular effects which govern the absorption and fluorescence properties of solvated molecular probes, such as solvent-induced structural modifications, polarization effects, solubility, solute−solvent hydrogen-bonding interactions, and solute aggregation. To this aim we have exploited a time dependent density functional theory (TDDFT) approach coupled to complementary solvation approaches (continuum, discrete and mixed discrete and continuum). Such an integration has allowed us to clearly disentangle the complex interplay between specific and nonspecific interactions of the solvent with the probes and show that strong H-bonding effects not only can lead to large solvatochromic shifts but also can affect the nature of the emitting species with resulting reduction of the quantum yield.

1. Introduction

Solvatochromic shifts are commonly exploited as simple univocal indices to classify the environment, but, in reality, they reflect extremely complex phenomena involving many different intermolecular forces and being affected by coupled dynamical processes of both the molecular probe and the solvent.[1] This is more evident in emission spectra because the environment effects not only influence the energy of the excited state but also govern which state has the lowest energy. In particular, in the emission process, the spectroscopic measurement defining the solvatochromism cannot be separated from the dynamics of the excited molecular probe and of the solvent around it. Very different situations can exist: the excited probe may remain immobilized at a certain location, or, in the opposite scenario, due to molecular diffusion, it may undergo excursion over a distance within its excited-state lifetime and, as a result, it will report the average property of a region a few nanometers in radius. On the other hand, solvent molecules can remain frozen in their orientational distribution determined by the initial equilibrium situation with the probe in its ground state, or, on the contrary, they can partially or completely rearrange toward a new equilibrium with the excited probe in its excited state. All these different situations will strongly affect the spectroscopic emission signal of the probe both in terms of the position and the shape of the peak as well as by inducing enhancement or quenching.[2]

Due to all these aspects, a molecular probe will be able to show evident solvatochromism if it presents specific characteristics which make its intermolecular interactions extremely sensitive to even small changes in the environment. Molecular systems which present these characteristics are the so-called charge-transfer (CT) probes, i.e., those systems in which the excitation process can be rationalized in terms of an intramolecular charge transfer from one part of the molecule (the donor part) to another part (the acceptor part). Commonly CT probes are characterized by donor (D) and acceptor (A) chromophores connected by conjugated or aromatic bridges. The CT probes are extremely sensitive to the environment for what concerns both their local and bulk properties; in fact, during the excitation process the changes in the charge distribution lead to large changes in the dipole moment which, in turn, strongly modify the interactions with the environment. If the CT probe also presents hydrogen-bonding (HB) sites the excitation process will induce further modifications, this time in the local environment, which will make the spectroscopic signal very sensitive to HB properties of solvents in addition to polarity. In particular, femtosecond-resolved fluorescence Stokes shifts have shown that the charge transfer within HB system is assisted by collective solvent interactions and the delocalization of charges through the network.[3] In addition, the possibility for CT excited state to activate HB networks can give rise also to new deactivation channels mostly of nonradiative nature, which can largely reduce the fluorescence quantum yield and eventually lead to its complete quenching.[4] The goal of this paper is to give a microscopic explanation of this complex phenomenon of solvatochromism and of the related solvent effects on the deactivation process of fluorescence. To achieve such a detailed analysis, a quantum-mechanical (QM) simulation of the investigated absorption and emission processes using a combination of different computational models will be performed. In particular, three alternative families of methods for evaluating the solvent effects will be used (a polarizable continuum model, PCM,[5] a combined molecular dynamics (MD) and QM/polarizable molecular mechanics (MM) approach,[6] and a "supermolecular" approach where both the solute and some neighboring solvent molecules are explicitly included in the QM calculations. These methods will be applied to the study of both absorption and fluorescence of a set of representative CT systems (see Figure 1), namely, 4-aminophthalimide (4-AP),

* To whom correspondence should be addressed. E-mail: bene@dcci.unipi.it.

10.1021/jp1097487
Published on Web 12/03/2010

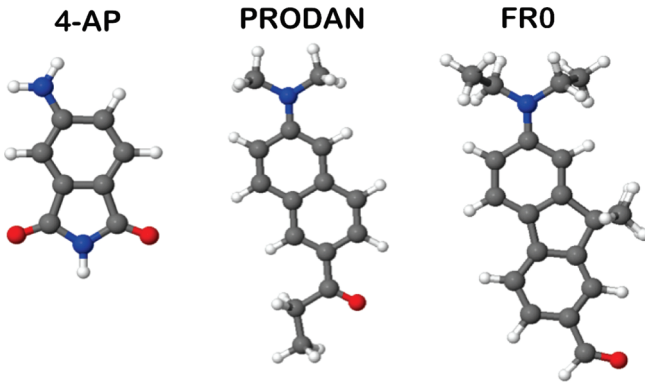

Figure 1. Graphical representation of the three investigated molecules.

6-propionyl-2-dimethylamino naphthalene (PRODAN), and its recently synthesized analogue 7-diethylamino-9,9-dimethyl-9*H*-fluorene-2-carbaldehyde (FR0).

The paper is organized as follows: in the section Methodological Aspects a brief overview of the computational methods used is given together with some comments on the correct modeling of the response of the solvent to the excitation−dexcitation processes. In the Results and Discussion section the analysis is presented in terms of separated subsections on (i) the nature of the excited states, (ii) the solvatochromic shifts predicted by continuum media, (iii) the short-range solvents effects on the photophysical processes described using molecular dynamics and supermolecule (or cluster) approaches, and (iv) the solvent effects on quantum yields.

2. Methodological Aspects

2.1. Computational Details. All the QM calculations have been performed by using a locally modified version of the Gaussian 09 package.[7] The ground- (GS) and first singlet excited-state (ES) geometry optimizations and absorption and emission calculations were performed by means of the (TD)DFT method using the CAM-B3LYP functional[8] and the 6-311+G(d,p) basis set. The integral equation formalism (IEF)[9] version of PCM has been used to describe the effects of the environment with cavities built as a series of interlocking spheres centered on atoms with the following radii:[10] 1.7 Å for C, 1.9 Å for CH, 2.0 Å for CH_n (n = 2, 3), 1.52 Å for O, 1.6 Å for N, and 1.2 Å for H not bonded to C, all multiplied by a cavity size factor of 1.2. PCM vertical absorption and emission energies were obtained, by exploiting the corrected linear response (cLR) scheme.[11] To analyze the effects of hydrogen bonding, molecular dynamics (MD) simulations were carried out with two protic solvents (water and methanol). Solute geometries are the same optimized structures previously used for the absorption and emission calculations. During all the simulations, the solute geometry was kept fixed. Every solute was inserted in parallelepiped boxes and solvated with nonpolarizable TIP3P water molecules[12] and nonpolarizable f99 methanol molecules.[13] All the simulations were performed using the AMBER9 package where the solute was described with the general amber force field (GAFF).[14] In order to extend the simulations to excited states and to have a consistent picture for both GS and ES simulations, the electrostatic charges have been calculated with the Merz−Singh−Kollman scheme[15] applied to GS and ES geometry and electronic density, respectively, using the same level used for the QM calculations. Before each production simulation was started, the cell size for both adducts was adjusted in a series of minimizations and short NVT molecular dynamics simulation runs in order to achieve both the correct temperature of the MD bath and the correct density of the solvent molecules filling the simulation box. The final box dimensions and the corresponding number of solvent molecules are collected in Table S.1 of the Supporting Information. The Andersen temperature coupling scheme[16] with a relaxation time of 0.4 ps was employed. The time step was set to 1 fs. Periodic boundary conditions were applied, and the particle mesh Ewald method[17] was used to deal with electrostatic forces. Starting from the last obtained equilibrium configuration, production runs were performed in the NVT ensemble for a total simulation time of 2 ns. Mean residence times have been calculated according to the Garcia and Stiller algorithm.[18] The exponential survival function was obtained as the average of 20 000 configurations, that is, every 0.1 ps. Configurations were saved every picosecond for subsequent QM and QM/MMpol calculations.[6d] New sets of partial atomic charges and distributed polarizabilities were derived and used in the QM/MMpol calculations (see Table S.2 and S.3). In particular, the distributed atomic dipole−dipole polarizabilities were calculated using the LoProp[19] approach as implemented in the Molcas[20] program, whereas the atomic charges were fitted to the electrostatic potential following the ESP method implemented in the GAUSSIAN package. For a more detailed discussion, see ref 21. The calculations were performed at B3LYP/aug-cc-pVTZ level. The ground- and excited-state geometry optimizations of aromatic dimers were calculated with the (TD)DFT method using the M06-2X functional[22] with the 6-311+G(d,p) basis set. In all cases absorption and emission energies were computed with CAM-B3LYP.

2.2. Considerations about Solvent Nonequilibrium. The full process of formation and relaxation of the excited state is generally simplified in terms of three sequential time steps: (i) vertical excitation, (ii) nuclear relaxation in the electronically excited state, and (iii) vertical emission toward the vertical ground state. In the presence of a polarizable environment, the three steps are characterized by three specific solvent responses which measure the collective polarization of all the solvent molecules. In the more interesting case of a polar solvent, the polarization consists of two parts: electronic and orientational. The electronic polarization is nearly instantaneous while the orientational polarization is much slower and occurs at a time scale that ranges from a few picoseconds for the reorientation of a small −OH group (like in alcohols and in water) to a few microseconds on a large macromolecular chain.[23] When the probe solute is excited, the solvent dipoles initially (i.e., at t = 0) remain oriented about the ground-state solute charge distribution, and the potential energy of the excited solute is high. With an increase in time, the solvent dipoles gradually reorient and the energy of the system decreases until the probe decays toward the ground state emitting the fluorescence radiation. Once again, in this fast radiative process, the electronic polarization instantaneously relaxes whereas the solvent dipoles remain oriented in their initial (i.e., excited-state-induced) configuration. These delays in the solvent response, also known as nonequilibrium effects, have to be properly included in the calculations of both absorption and emission energies. Using a PCM approach, they are taken into account partitioning the surface charges into a fast (or electronic) and a slow (or inertial) component and assuming from them a different response time: instantaneous for the former one and of the same time scale of that characterizing the nuclear relaxation of the excited state for the other. To fully account for these nonequilibrium effects in a MM description of the solvent, a polarizable force field is

TABLE 1: Ground-State (GS), Excited-State (ES), and Ground-to-Excited-State (ES−GS) Change of Dipole Moments Determined by Various Authors Using Several Methods[a]

	calcd	exptl
		4-AP
μ^{GS}	5.3 (7.0)	3−4 (ref 26)
$\Delta\mu$(ES−GS)	4.5 (8.0)	3−5 (ref 26)
		PRODAN
μ^{GS}	6.0 (4.6)	3 (ref 31); 5 (refs 27−29)
$\Delta\mu$(ES−GS)	8.5 (9.2)	5 (ref 28); 7 (ref 27); 8 (ref 31); 13 (ref 29); 20 (ref 30)
		FR0
μ^{GS}	6.8 (9.1)	−
$\Delta\mu$(ES−GS)	7.3 (13.5)	14 (ref 32)

[a] The calculated values refer to calculations performed in gas phase (and in a PCM polar solvent). All values are in debye.

necessary. In fact in standard nonpolarizable MM, delays in the orientational polarization are accounted for by keeping the MM molecules in the configuration determined by a MD simulation performed for the probe in the initial electronic state (GS for absorption and ES for emission), while the fast component of the polarization is completely neglected. In a polarizable MM approach, on the contrary, the presence of induced dipoles in addition to fixed MM atomic charges allows for the inclusion of the fast component of the polarization.

3. Results and Discussion

To proceed in the following investigation of the molecular properties of the investigated probes, a preliminary conformational analysis is necessary. For symmetry reasons 4-AP possess only a conformation, whereas PRODAN and FR0 (shown in their *cf.*1 state in Figure 1) have another accessible conformational state (*cf.*2, with the C═O group flipped 180° with respect to the aromatic plane) in both their ground and excited states. Our calculations show that PRODAN and FR0 *cf.*1 are slightly more stable than the corresponding *cf.*2 (about 0.4 kcal/mol in water for PRODAN and about 0.2 in methanol for FR0) at the GS. In the following analysis the focus will therefore be focused on *cf.*1, but checks on possible specificities due to the presence of the other conformer were taken into account.

3.1. Considerations about the Nature of Ground and Excited States. The pronounced solvatochromism of molecules characterized by donor and acceptor groups connected through conjugated π-bonds is mainly due to a net change in the charge distribution (see Figure S.2) moving from the electronically ground to the excited state.[2] Such a charge transfer is quantified in terms of a large change in dipole moment in the excited states. Table 1 collects experimentally determined ground-state dipole moments and the ground-to-excited changes,[24−32] together with the results calculated in the present work. Calculated (TD)DFT values for 4-AP are in good agreement with experiments[26] when gas-phase data are considered; this is what one should expect as the experimental data are generally extrapolated at zero polarity. As far as PRODAN is concerned, a more delicate analysis is required as a long-term controversy is whether PRODAN fluorescence occurs from a planar or from a twisted state.[24] Abelt and co-workers[25] investigated the photophysical properties of several PRODAN derivatives, where the dialkylamino group is constrained to be planar or perpendicular with the naphthalene ring, by means of experimental solvatochromism studies. They found that constrained planar analogues behave just like PRODAN, while twisted analogues behave very differently, and, in addition, they have a pyramidal amino group rather than one that is planar. All this considered, they concluded that PRODAN emission is from a planar intramolecular charge-transfer state. This conclusion is further confirmed here on the basis of values reported in Table 1 for the variation of the dipole moment.

Contrary to what originally reported by Weber and Farris[29] who found a large (20 D) variation of the dipole moment upon excitation, the successive experimental analyses have shown that the variation of the dipole of PRODAN is in line with other CT systems, being in the range 4−9 D. Indeed a trivial error in the equation used by Weber and Farris was recognized by Balter et al.,[31] who corrected the dipole variation to only 8 D from an analysis of solvatochromic data in some selected solvents. The calculated (TD)DFT values (4.6−9.3 D) are in agreement with these most recent experimental data, and they show that a planar ES state structure indeed provides a reliable description of the excited-state dipole moment of PRODAN in both apolar and polar environments.

As far as the recently synthesized FR0 system is concerned, the value of the ground-to-excited-state change of dipole moment, $\Delta\mu$(ES−GS), determined by Kucherak et al.[32] is in very good agreement with that calculated at the (TD)DFT level in polar solvent.

In conclusion, the selected QM level of calculation [(TD)-CAM-B3LYP] seems to correctly reproduce the electronic and geometrical changes following the excitation for all the three molecules. This makes us confident that a similar reliability of such a method also applies to the analysis of solvent-induced changes.

3.2. Analysis of the Experimental Data. Before moving to the results, it is necessary to make a preliminary analysis on the use of available experimental data. As gas-phase data are usually difficult to be experimentally determined, it is necessary to introduce as reference the most "inert" apolar solvent among those measured. Here the term inert means that the selected solvent, besides being apolar, should not present any specific interaction with the solute and should also allow a good solubility. For PRODAN and FR0, the most standard apolar solvent, namely hexane, seems not a good choice. Both molecular probes show in fact a very low quantum yield in hexane and an unexpected blue shift with respect to other apolar solvents (with respect to dioxane and toluene 0.2−0.4 eV blue shifts are observed in the fluorescence). These shifts indicate possible aggregation effects due to the high polar character of the probes and their low solubility in hydrocarbon solvents.[33] If now we assume that this effect is active also in PRODAN when dissolved in hexane, we can relate the blue shift observed in the fluorescence to the formation of dimers in the excited state reasonably stable in the low polar hexane. To test such a hypothesis we have considered a PRODAN dimer assuming a stacked structure with an antiparallel arrangement. The final optimized structure for the excited state is shown in Figure 2.

The calculated shift in the dimer fluorescence with respect to the monomer value is 0.16 eV toward the blue, whereas the shift derived from the difference in fluorescence maxima measured in hexane and in dioxane or in toluene is ca. 0.2 eV. As it can be seen from this comparison, the aggregation effects correctly reproduce the experimentally observed blue shift, and they confirm that hexane cannot be considered as an inert solvent. For PRODAN and FR0 probes, we have thus selected dioxane as inert reference solvent.

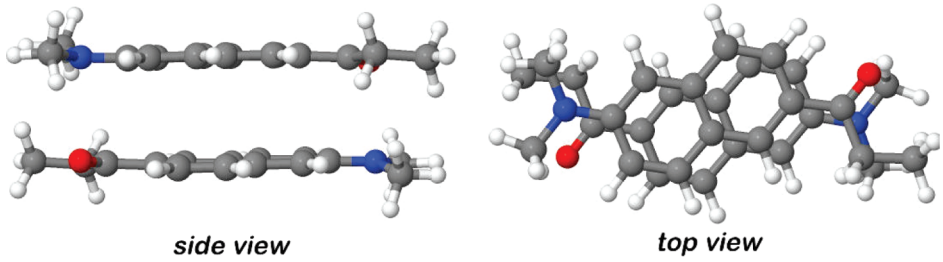

Figure 2. Structure of the antiparallel dimer of PRODAN in its side (left) and top (right) views. The distance between the aromatic planes is 3.09 Å, and the monomer units are slightly (of about 0.7 Å) translated with respect to one another.

TABLE 2: Comparison between Experimental and PCM Solvent-Induced Shifts on Absorption (Abs) and Emission (Flu) Energies (eV) and Stokes Shift (SS) (cm^{-1}) of the Three Selected Probes[a]

	4-AP			PRODAN			FR0	
	δ_{pol}	δ_{HB}		δ_{pol}	δ_{HB}		δ_{pol}	δ_{HB}
		MeOH	water		MeOH	water		MeOH
				Abs				
exptl	−0.19	−0.12	−0.13	−0.11	−0.06	−0.01	−0.03	−0.02
calcd	−0.15	0.00	−0.01	−0.05	0.00	−0.01	−0.07	0.00
				Flu				
exptl	−0.52	−0.31	−0.40	−0.25	−0.22	−0.30	−0.38	−0.20
calcd	−0.41	0.00	−0.03	−0.22	0.00	−0.02	−0.35	0.00
				SS				
exptl	2725	1534	2192	1161	1257	2310	2804	1485
calcd	2115	26	183	1339	15	115	2308	20

[a] δ_{pol} indicates the shift moving from hexane to acetonitrile for 4-AP and from dioxane to dimethylsulfoxide for PRODAN and FR0. Experimental data are taken from ref 34 for 4-AP and ref 32 for PRODAN and FR0.

3.3. A Purely Continuum Description. In Table 2 we report a comparison between experimental and calculated solvent-induced shifts on absorption (Abs) and emission (Flu) energies (eV) and Stokes shifts (SS) (cm^{-1}) of the three probes. The comparison is split into a δ_{pol} shift obtained moving from apolar (hexane for 4-AP, dioxane for PRODAN and FR0) to polar solvent (acetonitrile for 4AP and dimethylsulfoxide for PRODAN and FR0) and a further δ_{HB} shift obtained moving from the polar solvent to an hydrogen-bonding one (methanol and water for 4-AP and PRODAN and methanol for FR0). All calculated results refer to the PCM method.

For all probes the continuum description gives very accurate estimates of the polarity-induced δ_{pol} shift for both absorption and fluorescence energies and SS. The good general agreement found for δ_{pol} shifts is an important result. It in fact shows that nonelectrostatic effects (mostly due to dispersion and repulsion interactions between solute and solvent) which are not included in the PCM model are either not important in these systems or (more probably) quite insensitive to the solvent; thus, they cancel out when solvent−solvent shifts are considered. On the contrary, large discrepancies are observed on the additional δ_{HB} for all the probes: this is reasonably expected for continuum models, which do not accurately account for strong local effects as those induced by H-bonds. It is, however, important to note that δ_{HB} is quite different for absorption and fluorescence processes; indeed for fluorescence it is large for all probes (0.2−0.4 eV) while for absorption it is really relevant only for 4-AP (0.12−0.13 e.V). These findings show an important specificity of 4-AP with respect to the other probes, namely, its capacity to establish strong H-bond already at the electronic ground state. As a result of the unsatisfactory description of H-bonding effects on absorption/emission energies, the PCM-calculated SS are largely underestimated for all probes in all protic solvents. These behaviors will be further discussed in the following section where H-bonding effects will be analyzed combining different computational strategies.

3.4. Hydrogen Bonding and Other Structuring Effects. One of the most important questions to clarify is if the solvent molecules are able to do stable clusters that modify the optical properties of the solute. Such an analysis is made possible by using a classical MD simulation of each molecular system in the corresponding protic solvent (in water and in methanol solution, for both ground and excited states of 4-AP, in water for excited-state PRODAN, and in methanol for excited-state FR0). In Figure 3 the 3D radial distribution functions are shown for 4-AP in water in its ground (top left) and excited (top right) state and for excited states of PRODAN (bottom left) in water and of FR0 in methanol (bottom right).

Let us first focus the MD analysis on the 4-AP. As expected by the CT character of the excited state, the coordination number of each carbonyl group increases from 1.1 to 1.5 in water upon excitation. If we now consider the complete HB sensitive part of the molecule, the number of solvent molecules increases from 5 to 7 upon excitation. In parallel, the mean residence time (τ) at the carbonyl groups is increased from 10 to 20 ps. The change in the τ is even more important in the methanol solution, where the molecules remain 92 ps in the first solvation shell for the excited state. It is also worth noting that the O(AP)−H(solvent) distance for the excited state is smaller than the usual H-bonding distance (1.65 Å for both methanol and water solutions). All these data lead us to characterize the H-bond interactions in the excited 4-AP as a situation in between a standard H-bond and a real covalent bond.

Moving to PRODAN and FR0, the HB sensitive sites reduce to the carbonyl groups only. The corresponding coordination numbers are 1.4 (with 24 ps residence time) and 2.2 (and 103 ps) for PRODAN in water and FR0 in methanol, respectively. The methanol molecules around the solute form a much more rigid structure than the water ones, which, being smaller, have a larger motion freedom than the methanol.

Combining the previous PCM results and this MD analysis, the final picture that comes out for all the probes dissolved in protic solvents is the formation of strongly interacting excited solute−solvent aggregates. These supramolecular systems can be simulated using different strategies. Either one extracts a statistically meaningful sample of solute−solvent configurations from MD trajectories and uses them to simulate the process of interest, or one assumes that the interactions between the solute and the first-shell solvent molecules are so strong and so persistent in time that they really constitute a stable supermolecular system which can be characterized exactly as a real molecular system including its geometry which is obtained through a full QM optimization (Figure 4).

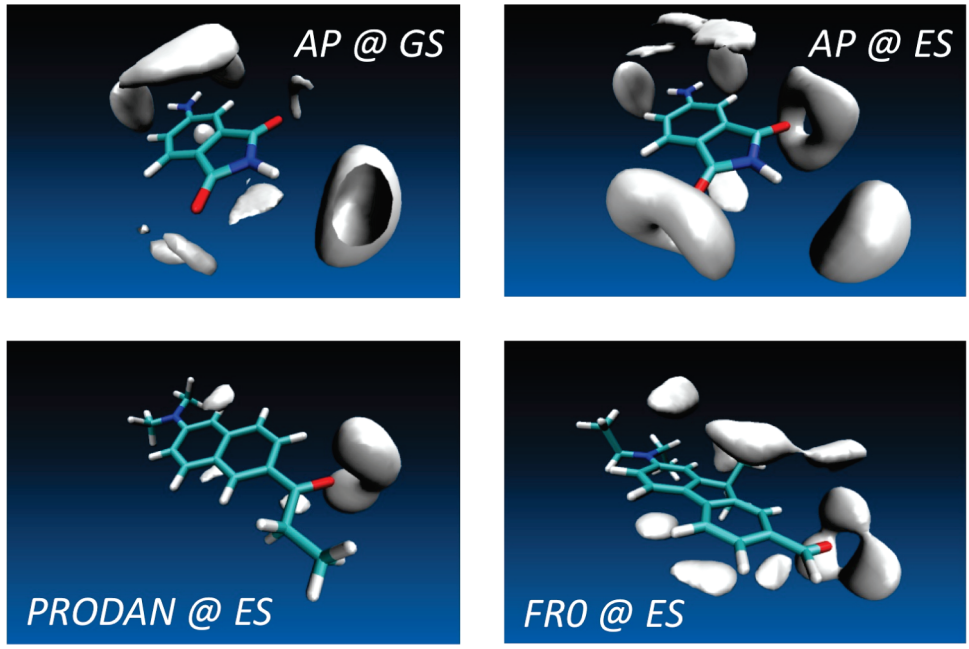

Figure 3. 3-D radial distribution functions solute−H(solvent) for 4-AP in water for the ground and excited states (GS and ES, respectively) and for the excited state of PRODAN in water and FR0 in MeOH.

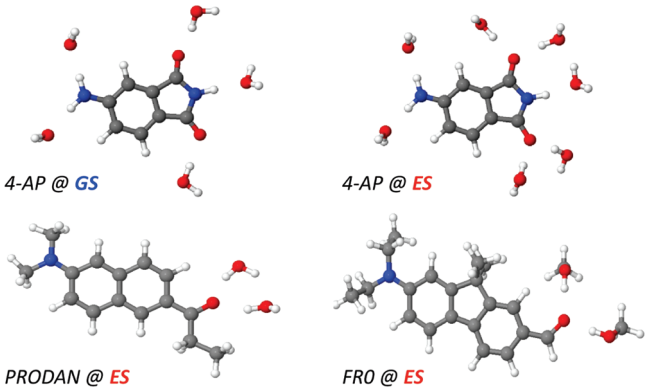

Figure 4. Structures of *supermolecular* systems of 4-AP (both in its ground and excited state) and PRODAN and FR0 (both in their excited states) obtained from QM optimizations of the solute surrounded by explicit HB solvent molecules.

Let us start the analysis of the two strategies with 4-AP. As said before for this probe both the absorption and the emission processes are significantly affected by H-bonds, and therefore MD simulations have been repeated for the two electronic states and the QM supermolecules have been calculated both in the ground and in the excited state. In Figure 5a we report the δ_{HB} values for both absorption and fluorescence in water obtained with the different solvation approaches and, in Figure 5b, the corresponding shifts on SS. Here the PCM values refer to those reported in Table 2. We note that two different supermolecule schemes have been tested. One (indicated as +nmol in the graphs) considers only H-bond effects, and therefore the optimization of the cluster as well as the following absorption and fluorescence calculations have been performed in the gas phase while another (PCM+nmol) also includes the effects due to the rest of the solvent beyond the first solvation shell by embedding the cluster in a PCM solvent; in this second scheme both the geometry optimization of the cluster and the abs/flu processes have been calculated including PCM effects. Also in the case of MD-derived clusters two different schemes have been tested. In the first scheme we have selected 100 configurations and introduced a cutoff of 12 and 14 Å for water and methanol, respectively, and on the resulting aggregates we have applied a QM description for the probe and a polarizable MM for all the solvent molecules. The resulting average is indicated as ⟨MD+MMpol⟩ in the graphs. The second scheme still uses the same MD-derived configurations, but it introduces a shorter cutoff (2.2 Å) and the resulting by far smaller clusters are described using a QM level for both the probe and the solvent molecules whereas the rest of the solvent is substituted by PCM. The resulting average is indicated as ⟨MD-PCM⟩. Due to the much larger computational cost of this second approach, the average has been limited to 20 configurations.

The first important result which comes out is that both descriptions based on only mean-field effects (PCM) or only H-bonds (+nmol) poorly reproduce the measured shifts. Only in the case of absorption, H-bond effects seem to be dominant and +nmol results are in sufficient agreement with experiments, but this is not true for emission for which pure H-bond effects catch only a minor percentage of the full shift. As a result of this asymmetry in the two processes, the shift on SS is wrong both qualitatively and quantitatively. By adding the effects of the rest of the solvent molecules with a PCM approach, the picture changes drastically: the shift on emission is correctly reproduced whereas some discrepancies remain for the absorption process for which PCM+nmol overestimates the shift, and, as a result, the shift on SS is underestimated. The overestimation in the shift for the absorption process seems to show that a single PCM-QM cluster is not representative of the more dynamic behavior of the solvent molecules around the ground-state solute. This hypothesis is confirmed by the accurate picture obtained with MD-derived solute−solvent configurations treated at the QM/MMpol level of description. In this case, both the absorption and the emission processes and the final SS are correctly reproduced. Finally, it is worth remarking that the different behaviors of the various solvation models for absorption and fluorescence energies have to be seen as due to quite different solvation dynamics for the ground and the excited state. While for excited state, all models are equally accurate in reproducing the observed δ_{HB} shift, this is not true for absorption. In other words, this can be expressed saying that the H-bonding effects

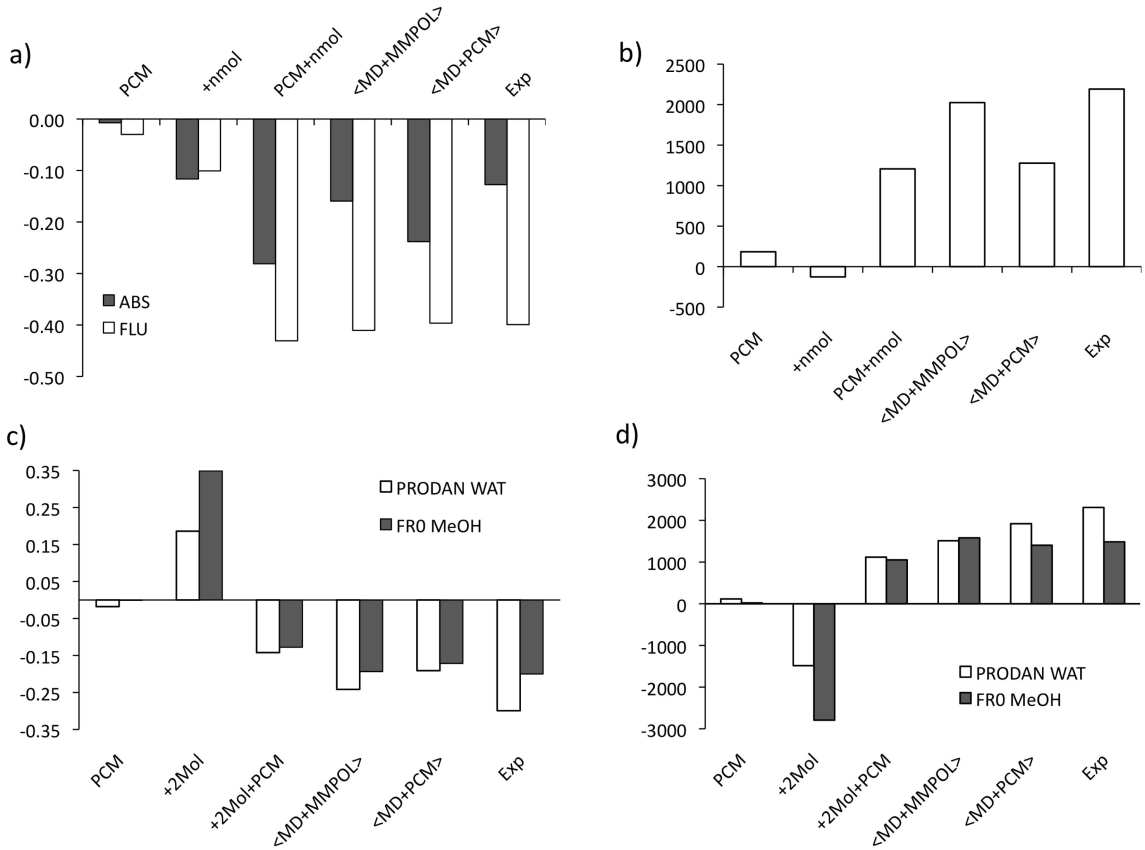

Figure 5. Calculated and experimental (a) absorption and emission δ_{HB} and (b) δ_{SS} for 4-AP moving from the polar solvent to water; (c) emission δ_{HB} and (d) δ_{SS} for PRODAN and FR0 moving from the polar solvent to the protic one (water for PRODAN and methanol for FR0). δ_{HB} values are in eV and δ_{SS} in cm^{-1}. The labels "+nmol" and "PCM+nmol" refer to values obtained on the QM supermolecules shown in Figure 4.

on the excited state are so strong and so persistent in time that we are exactly in the limiting case where the static picture kept by PCM+nmol and the dynamic one kept by ⟨MD+MMpol⟩ coincide. For the 4-AP in the ground state instead, H-bond effects are weaker and their description requires a real dynamic approach.

The computational analysis can go even further in investigating the role of H-bonding effects. It can, for example, dissect the behavior of the various sensitive sites of 4-AP and verify if they are additive. To reach this goal, we have considered the dimethylamino version of the AP probe (DAP). Due to the methyl substitution, DAP presents a lower capacity to attract water molecules with respect to 4-AP, and, if H-bonding effects are additive, it should have a smaller δ_{HB} for both absorption and emission. Indeed this is not the case as the measured δ_{HB} is around 0.15 eV for absorption and 0.3 eV for emission in both 4-AP and DAP. To have a definitive proof that this experimental observation is an indication of the dominant role played by H-bonds with carbonyl oxygen atoms, we have determined a new QM supermolecule, constituted by excited-state DAP and five water molecules. The structure we have considered is parallel to the one used for 4-AP (see Figure 4) but without the two further water molecules H-bonded to NH_2 group. In addition, we have included the effect of the rest of the water molecules using PCM. The δ_{HB} calculated for DAP supermolecule moving from acetonitrile to water is in very good agreement with experiments (0.31 eV), and this confirms what suggested by the experimental observation, i.e., the dominant role played by carbonyl oxygens in the interaction with water molecules.

Moving to PRODAN and FR0, in Figure 5c−d we report exactly the same analysis shown for 4-AP, but this time only emission (c) and SS values (d) are reported as for absorption δ_{HB} is negligible. As can be seen from the graphs, the description based on only H-bond effects (+2 mol) is not only quantitatively insufficient but also qualitatively wrong as it leads to a blue shift instead of a red shift in the emission energies. This results shows that the δ_{HB} shift is the result of a balanced combination of specific H-bonds and longer-range effects. This is further confirmed by the good results obtained with any of the three approaches including the effect of the solvent outer shells. More in detail, the PCM-solvated QM clusters (PCM+2 mol) correctly reproduce the observed behaviors, but they slightly underestimate the shift for FR0 and more significantly for PRODAN; as a result, the shifts on SS are too low for both probes. On the contrary, the two MD-derived approaches (both PCM and MMPol) give a very good description for both probes, with PRODAN still presenting a small underestimation. Indeed the real physics beyond the large solvatochromism of PRODAN fluorescence and its specific sensitivity to H-bonding environments is a still open and very challenging problem as we have commented in the previous sections where we have summarized the debate on the possibility of twisted emitting species. However, from our study some conclusions can be derived. First of all, a twisted structure seems to be excluded in any solvent (either apolar, polar, or protic): for both apolar (but still inert) and polar solvents a PCM-like picture of a planar emitting system well reproduces the solvatochromism both in the absorption and in the emission process as well as correctly reproducing the high Stokes shifts. Moreover, specific effects due to solvent molecules which present a clear structured distribution around the excited state have shown to be fundamental to describe the additional shift observed in protic solvents. Once that is clarified, however, some further minor

but not negligible effects are still missing in order to completely simulate the solvatochromism of PRODAN. Here we try to suggest two possible mechanisms that could be active in the excited state of PRODAN.

The first possible mechanism has been proposed by Rowe et al.[35] for PRODAN based on a multivariate photokinetic analysis, and it suggests that excitation increases the probability of the carbonyl oxygen protonation in protic solvents. To verify if this hypothesis can indeed explain the large δ_{HB}, we have calculated the optimal geometry of possible protonated species, the PRODAN itself and the PRODAN with two H-bonded water molecules. For both structures we have calculated the emission energies: the resulting δ_{HB} shifts are very similar for the two species, and they are both ca. -0.5 eV. This value is clearly a large overestimation of the observed -0.3 eV but still indicates that effects due to strong H-bonds which eventually result in labile protonated species are in qualitative agreement with the experimental findings. Another possible mechanism that we propose here involves a conformational change induced by excitation. In a recent study[36] on a different probe, acetyl anthracene, we have shown the possibility for an isomerization, due to rotation of the carbonyl group, upon excitation. If we now assume that the same mechanism can be possible for PRODAN especially when dissolved in H-bonding solvents, we can verify if the emission properties of the second possible conformer (*cf.*2) can explain the missing contribution to the observed δ_{HB}. To do that we have determined the optimal geometry of the excited-state conformer obtained by a 180° rotation of the carbonyl group with respect to the aromatic plane and calculated the resulting emission energy. Such an analysis has been repeated for both the PRODAN and the PRODAN H-bonded to two water molecules; in both cases, bulk effects due to a PCM solvent have been introduced. The resulting structures present a larger stability than the corresponding ones obtained for *cf.*1 and an additional fluorescence δ_{HB} shift of -0.05 eV. This additional red shift if summed to the δ_{HB} found for the ⟨MD+MMPol⟩ model applied to *cf.*1 leads to a final HB shift of -0.29 eV, in very close agreement with the experimental -0.3 eV shift measured in water. This analysis is certainly incomplete as calculations of transition barriers as well real of the photochemical reaction path should be performed, but it is a promising hypothesis to explain the additional red shift in the PRODAN fluorescence in protic solvents. We finally note that assuming a similar isomerization effect for FR0 in methanol does not lead to any significant change: emission energies for *cf.*2 in fact differ from those obtained for *cf.*1 by less than 0.02 eV.

3.5. Quantum Yield and Quenching Effects. All the systems here studied present high absorption coefficient and high (in the range of 60−90%) fluorescence quantum yield (QY) for most of the solvents. However, all of them show a net decrease of their QY with protic solvents (and more specifically with water): 2% in 4-AP, 12% in PRODAN, and 3% in FR0. Moreover, a strong decrease of QY is also observed for PRODAN and FR0 in hexane (2% in PRODAN and 11% in FR0). The explanations for these behaviors may be different. In the previous section we have already presented and discussed aggregation effects that can be active for PRODAN (and FR0) in very low polar solvents such as hexane. There we have used these aggregation effects to explain the unexpected blue shift of fluorescence found in hexane with respect to other low polar solvents. The same effects can be used here to explain the strong reduction of QY in this solvent: in fact aggregation induces excitonic splittings that lead to low-lying dark states not present on the monomeric species. Such states can thus represent possible new decay channels as they can lose their excitation energy in a nonradiative way, for example, due to transfers to the environment. More difficult is instead the analysis of the reduction of QY due to protic solvents (and in particular water) which is common to all the three studied probes. Yuan and Brown[37] attributed the observed decrease in the QY of two 4-aminonaphthalimides derivatives in aqueous ethanol (relative to ethanol) to the quenching by the water molecules. According to this model, a cluster of some seven or eight water molecules is required to effect the quenching, possibly corresponding to the excitation of one quantum of a stretching mode in each water molecule. Harju et al.[38] and Mukherjee et al.[34] suggested that the abrupt decrease in the QY of 4-AP in protic solvents was due to the reduction in the ES−GS energy gap in the proton-transferred species. Also Noukakis and Suppan[39] focused their attention on the protonation degree of the carbonyl group(s) in the excited CT state of AP. The analysis reported in the previous section confirms the fundamental role played by strong HB interactions in the excited state of 4-AP which gives rise to stable large clusters. In particular clusters including up to seven H-bonded water molecules are required to get the correct shift in the fluorescence. This picture can also be used here as an indirect confirmation of the experimentally suggested hypothesis that H-bonds effects are the responsible for the reduction of fluorescence in water (and other protic solvents).

Moving to PRODAN, recently Moyano et al.[40] have used spectroscopic techniques and cyclic voltammetry to show that in water, it self-aggregates due to its low solubility. They have also shown that PRODAN molar extinction coefficient for the charge-transfer electronic absorption band diminishes dramatically in water upon increasing the concentration, which suggests that the intramolecular charge-transfer process is inhibited by aggregation. The results we have previously discussed for PRODAN dimer in hexane can be reconsidered here to support such an hypothesis; as said before the aggregation gives rise to low-lying dark excited states which can allow additional nonradiative decay channels not available when PRODAN is not aggregated. This is the quenching mechanism in H-aggregates made of homodimers.

Unfortunately, specific studies on the QY properties of FR0 are not available, but the similarity with PRODAN reported in the reference paper by Kucherak et al.[32] for hexane seems to indicate that what we have found for PRODAN with the dimeric study can be valid also for this analogue probe.

4. Conclusions

We have shown that solvatochromism is a complex phenomenon in which very different interactions play a role, each with its proper dynamics. Such a complexity has direct important consequences in the large use that solvatochromism has in many fields of chemical and biological research. In fact, a clear and univocal relation between the position of absorption or fluorescence maxima and the characteristics of the environment cannot be obtained using simplified solvation models or even more complex polarity scales. Indeed, a detailed analysis of the static and dynamic aspects of solvation should be taken into account. In this paper we have shown that a new interpretative and predictive strategy is obtained by combining TDDFT approaches with various solvation models. Using only a single type of solvation model (either a continuum approach or an atomistic one) is in fact necessarily limited not only in the quality of the results it can achieve but also in the completeness of the physical picture it can give. In this study we have tried

to show that it is the integration of different (and complementary) solvation models that can reveal the real nature of solvatochromism by directly relating it to the effects of the environment on the formation and relaxation of excited states. In particular, by combining MD and QM descriptions, as well as integrating QM/continuum with QM/polarizable MM and full QM descriptions of the absorption and emission phenomena, we have shown that even in the case of very common and largely studied fluorescent probes, the analysis of solvatochromism is far from being simple and univocal. Many are in fact the aspects which can play a role, and some of them are only indirectly linked to the polarity and/or H-bonding characteristics of the environment. For example, one cannot neglect solubility effects which can hide unexpected shifts in the spectroscopic responses due not to direct environment effects but to environment-induced aggregations. More important, specific solute−solvent effects such as H-bonds not only can lead to large shifts of both absorption and emission energies but also can affect the nature of the emitting species with resulting reduction of the quantum yield. For some of the investigated probes, we have shown that strong H-bonding effects could lead to protonation of the acceptor sites in the probe or conformational changes.

Supporting Information Available: A summary of the experimental measurements of each molecular probe investigated in the paper, graphs of the changes on selected bond lengths and atomic charges going from ground to excited state for 4-AP, PRODAN, and FR0, and tables of the box dimensions used in the MD simulations and of the charges and polarizabilities of water and methanol used for MMPol calculations. This material is available free of charge via the Internet at http://pubs.acs.org.

References and Notes

(1) (a) Reichardt, C. *Solvent and Solvent Effects in Organic Chemistry*, 3rd ed.; Wiley-VCH: Weinheim, 2002;. (b) Suppan, P.; Ghoneim, N. *Solvatochromism*; The Royal Society of Chemistry: Cambridge, 1997.

(2) (a) Lakowicz, J. R. *Principles of Fluorescence Spectroscopy*, 3rd ed.; Springer: New York, 2006. (b) Valeur, B. *Molecular Fluorescence: Principles and Applications*, Wiley-VCH: Weinheim, 2001.

(3) Mohammed, O. F.; Kwon, O.-H.; Othon, C. M.; Zewail, A. H. *Angew. Chem., Int. Ed.* **2009**, *48*, 6251.

(4) (a) Flom, S. R.; Barbara, P. F. *J. Phys. Chem.* **1985**, *89*, 4489. (b) Nishiya, T.; Yamauchi, S.; Hirota, N.; Baba, M.; Hanazaki, I. *J. Phys. Chem.* **1986**, *90*, 5730. (c) Furstenberg, A.; Vauthey, E. *Photochem. Photobiol. Sci.* **2005**, *4*, 260. (d) Krystkowiak, E.; Dobek, K.; Maciejewski, A. J. *Photochem. Photobiol. A* **2006**, *184*, 250. (e) Sherin, P. S.; Grilj, J.; Tsentalovitch, Y. P.; Vauthey, E. *J. Phys. Chem. B* **2009**, *113*, 4953.

(5) (a) Tomasi, J.; Persico, M. *Chem. Rev.* **1994**, *94*, 2027. (b) Cramer, C. J.; Truhlar, D. G. *Chem. Rev.* **1999**, *99*, 2161. (c) Orozco, M.; Luque, F. J. *Chem. Rev.* **2000**, *100*, 4187. (d) Tomasi, J.; Mennucci, B.; Cammi, R. *Chem. Rev.* **2005**, *105*, 2999.

(6) (a) Thompson, M. A.; Schenter, G.K. *J. Phys. Chem.* **1995**, *99*, 6374. (b) Gao, J. L. *J. Comput. Chem.* **1997**, *18*, 1061. (c) Osted, A.; Kongsted, J.; Mikkelsen, K. V.; Åstrand, P.-O.; Christiansen, O. *J. Chem. Phys.* **2006**, *124*, 124503. (d) Curutchet, C.; Muñoz-Losa, A.; Monti, S.; Kongsted, J.; Scholes, G. D.; Mennucci, B. *J. Chem. Theory Comput.* **2009**, *5*, 1838.

(7) Frisch, M. J.; et al. *Gaussian 09*, revision A.1; Gaussian Inc.: Wallingford CT, 2009.

(8) (a) Yanai, T.; Tew, D. P.; Handy, N. C. *Chem. Phys. Lett.* **2004**, *393*, 51. (b) Chiba, M.; Tsuneda, T.; Hirao, K. *J. Chem. Phys.* **2006**, *124*, 144106.

(9) (a) Cancès, E.; Mennucci, B.; Tomasi, J. *J. Chem. Phys.* **1997**, *107*, 3032. (b) Mennucci, B.; Cancès, E.; Tomasi, J. *J. Phys. Chem. B* **1997**, *101*, 10506.

(10) Bondi, A. *J. Phys. Chem.* **1964**, *68*, 441.

(11) Caricato, M.; Mennucci, B.; Tomasi, J.; Ingrosso, F.; Cammi, R.; Corni, S.; Scalmani, G. *J. Chem. Phys.* **2006**, *124*, 124520.

(12) Jorgensen, W. L.; Chandrasekhar, J.; Madura, J. D.; Impey, R. W.; Klein, M. L. *J. Chem. Phys.* **1983**, *79*, 926.

(13) Cornell, W. D.; Cieplak, P.; Bayly, C. I.; Gould, I. R.; Merz, K. M.; Ferguson, D. M.; Spellmeyer, D. C.; Fox, T.; Caldwell, J. W.; Kollman, P. A. *J. Am. Chem. Soc.* **1995**, *117*, 5179.

(14) Case, D. A.; Darden, T. A.; Cheatham, T. E. I.; Simmerling, C. L.; Wang, J.; Duke, R. E.; Luo, R.; Merz, V.; Pearlman, D. A.; Crowley, V; Walker, R. C.; Zhang, W.; Wang, B.; Hayik, S.; Roitberg, A.; Seabra, G.; Wong, K. F.; Paesani, F.; Wu, X.; Brozell, S.; Tsui, V.; Gohlke, H.; Yang, L.; Tan, C.; Mongan, J.; Hornak, V.; Cui, G.; Beroza, P.; Mathews, D. H.; Schafmeister, C.; Ross, W. S.; Kollman, P. A. *AMBER 9*, 9th ed.; University of California: San Francisco, CA, 2006.

(15) (a) Singh, U. C.; Kollman, P. A. *J. Comput. Chem.* **1984**, *5*, 129. (b) Besler, B. H.; Merz Jr, K. M.; Kollman, P. A. *J. Comput. Chem.* **1990**, *11*, 431.

(16) Andersen, H. C. *J. Chem. Phys.* **1980**, *72*, 2384.

(17) Darden, T.; York, D.; Pedersen, L. *J. Chem. Phys.* **1993**, *98*, 10089.

(18) Garcia, A. E.; Stiller, L. *J. Comput. Chem.* **1993**, *14*, 1396.

(19) Gagliardi, L.; Lindh, R.; Karlström, G. *J. Chem. Phys.* **2004**, *121*, 4494.

(20) Karlström, G.; Lindh, V.; Malmqvist, P. Å.; Roos, B. O.; Ryde, U.; Veryazov, V.; Widmark, P.-O.; Cossi, M.; Schimmelpfennig, B.; Neograd y, P.; Seijo, L. *Comput. Mater. Sci.* **2003**, *28*, 222.

(21) Singh, U. C.; Kollman, P. A. *J. Comput. Chem.* **1984**, *5*, 129–145.

(22) Zhao, Y.; Truhlar, D. G. *Theor. Chem. Acc.* **2008**, *120*, 215–241.

(23) Nandi, N.; Bhattacharyyya, K.; Bagchi, B. *Chem. Rev.* **2000**, *100*, 2013.

(24) (a) Ilich, P.; Prendergast, F. G. *J. Phys. Chem.* **1989**, *93*, 4441. (b) Parusel, A. B. J.; Schneider, F. W.; Köhler, G. *J. Mol. Struct. (THEOCHEM)* **1997**, *398−399*, 341. (c) Mennucci, B.; Caricato, M.; Ingrosso, F.; Cappelli, C.; Cammi, R.; Tomasi, J.; Scalmani, G.; Frisch, M. J. *J. Phys. Chem. B* **2008**, *112*, 414.

(25) (a) Davis, B. N.; Abelt, C. J. *J. Phys. Chem. A* **2005**, *109*, 1295. (b) Everett, R. K.; Nguyen, H. A. A.; Abelt, C. J. *J. Phys. Chem. A* **2010**, *114*, 4946.

(26) (a) Ware, W. R.; Lee, S. K.; Brant, G. J.; Chow, P. P. *J. Chem. Phys.* **1971**, *54*, 4729. (b) Hagan, T.; Pilloud, D.; Suppan, P. *Chem. Phys. lett.* **1987**, *139*, 499. (c) Saroja, G.; Soujanya, T.; Ramachandram, B.; Soujanya, T.; Fessenden, R. W.; Samanta, A. *J. Phys. Chem.* **1996**, *100*, 3507.

(27) Catalan, J.; Perez, P.; Laynez, J.; Blanco, F. G. *J. Fluoresc.* **1991**, *1*, 215.

(28) Samanta, A.; Fessenden, R. W. *J. Phys. Chem. A* **2000**, *104*, 8972.

(29) Nemkovich, N. A.; Baumann, W. *J. Photochem. Photobiol., A* **2007**, *185*, 26.

(30) Weber, G.; Farris, F. J. *Biochemistry* **1979**, *18*, 3075.

(31) Balter, A.; Nowak, V.; Pawelkiewicz, W.; Kowalczyk, A. *Chem. Phys. Lett.* **1988**, *143*, 565.

(32) Kucherak, O. A.; Didier, P.; Mely, Y.; Klymchenko, A. S. *J. Phys. Chem. Lett.* **2010**, *1*, 616.

(33) Cohen, B. E.; Pralle, A.; Yao, X.; Swaminath, G.; Gandhi, C. S.; Jan, Y. N.; Kobilka, B. K.; Isacoff, E. Y.; Jan, L. Y. *Proc. Natl. Acad. Sci.* **2005**, *102*, 965.

(34) Mukherjee, S.; Sahu, K.; Roy, D.; Mondal, S. K.; Bhattacharyya, K. *Chem. Phys. Lett.* **2004**, *384*, 128.

(35) Rowe, B. A.; Roach, C. A.; Lin, J.; Asiago, V.; Dmitrenko, O.; Neal, S. L. *J. Phys. Chem. A* **2008**, *112*, 13402.

(36) Marini, A.; Muñoz-Losa, A.; Pucci, A.; Ruggeri, G.; Mennucci, B. *Phys. Chem. Chem. Phys.* **2010**, *12*, 8999.

(37) Yuan, D.; Brown, R. G. *J. Phys. Chem. A* **1997**, *101*, 3461.

(38) (a) Harju, T. O.; Huizer, A. H.; Varma, C. A. G. O. *Acta Chem. Scand.* **1995**, *49*, 829. (b) Harju, T. O.; Huizer, A. H.; Varma, C. A. G. O. *Chem. Phys.* **1995**, *200*, 215.

(39) Noukakis, D.; Suppan, P. *J. Lumin.* **1991**, *47*, 285.

(40) (a) Moyano, F.; Biasutti, M. A.; Silber, J. J.; Correa, N. M. *J. Phys. Chem. B* **2006**, *110*, 11838. (b) Moyano, F.; Molina, P. G.; Silber, J. J.; Sereno, L.; Correa, N. M. *Chem. Phys. Chem.* **2010**, *11*, 236.

JP1097487